Electronic Supplementary Material (ESI) for RSC Advances.

Supporting Information

Efficient blue electroluminescence with external quantum efficiency of 9.20% and CIE_y < 0.08 without excimer emission

Jayaraman Jayabharathi*, Sekar Sivaraj, Venugopal Thanikachalam, Balu Seransenguttuvan

Department of Chemistry, Annamalai University, Annamalainagar, Tamilnadu- 608 002, India, Email: jtchalam2005@yahoo.co.in

Address for correspondence

Dr. J. Jayabharathi
Professor of Chemistry
Department of Chemistry
Annamalai University
Annamalai nagar 608 002
Tamilnadu, India.
Tel: +91 9443940735
E-mail:jtchalam2005@yahoo.co.in

Contents:

SI-I: Scheme S1. Synthetic route of emissive materials

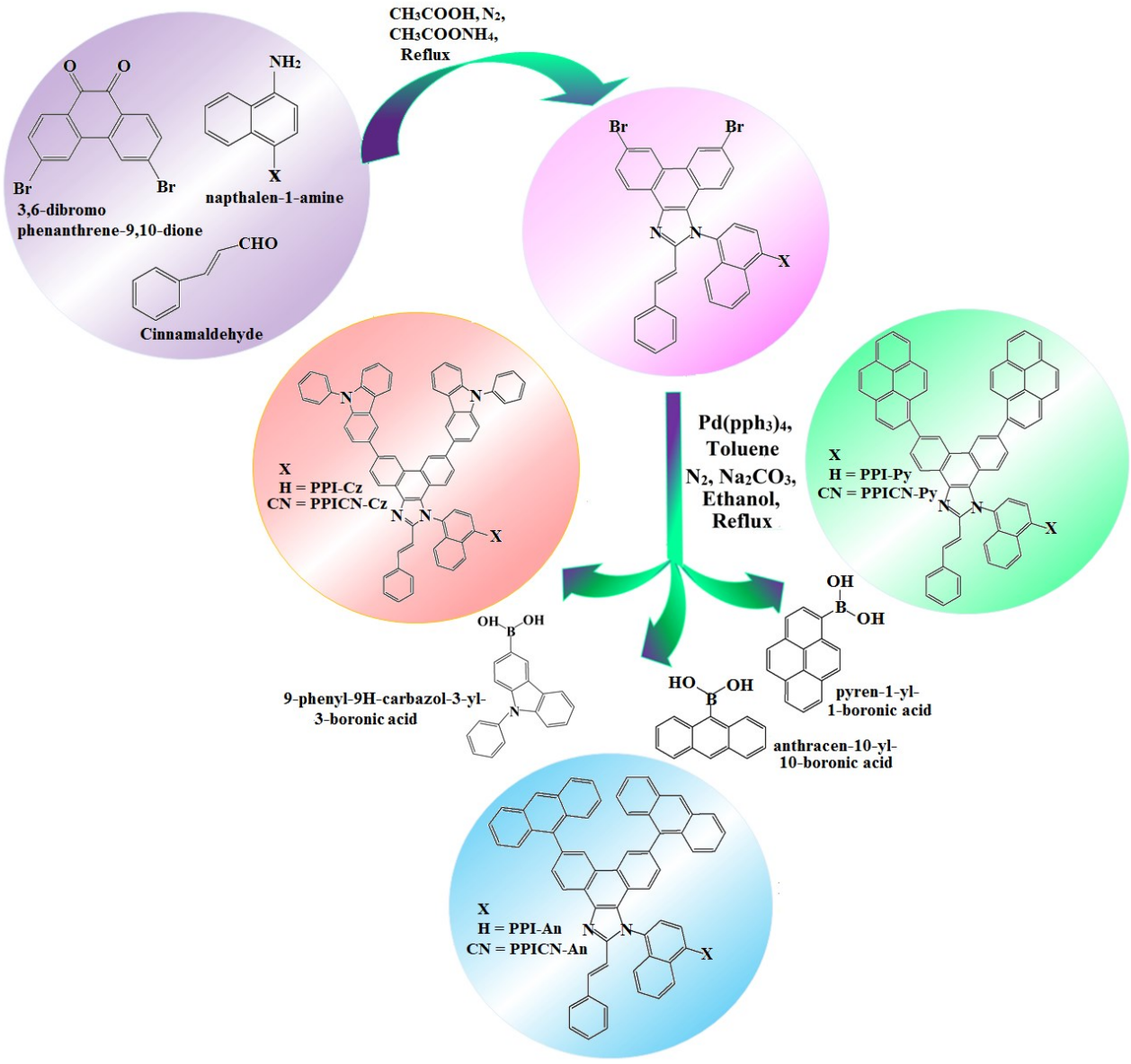

SI-II: Spectra of emissive materials (Schemes S2-S4)

Scheme S2. Spectra of (a)**PPI-Cz**; (b) **PPICN-Cz**

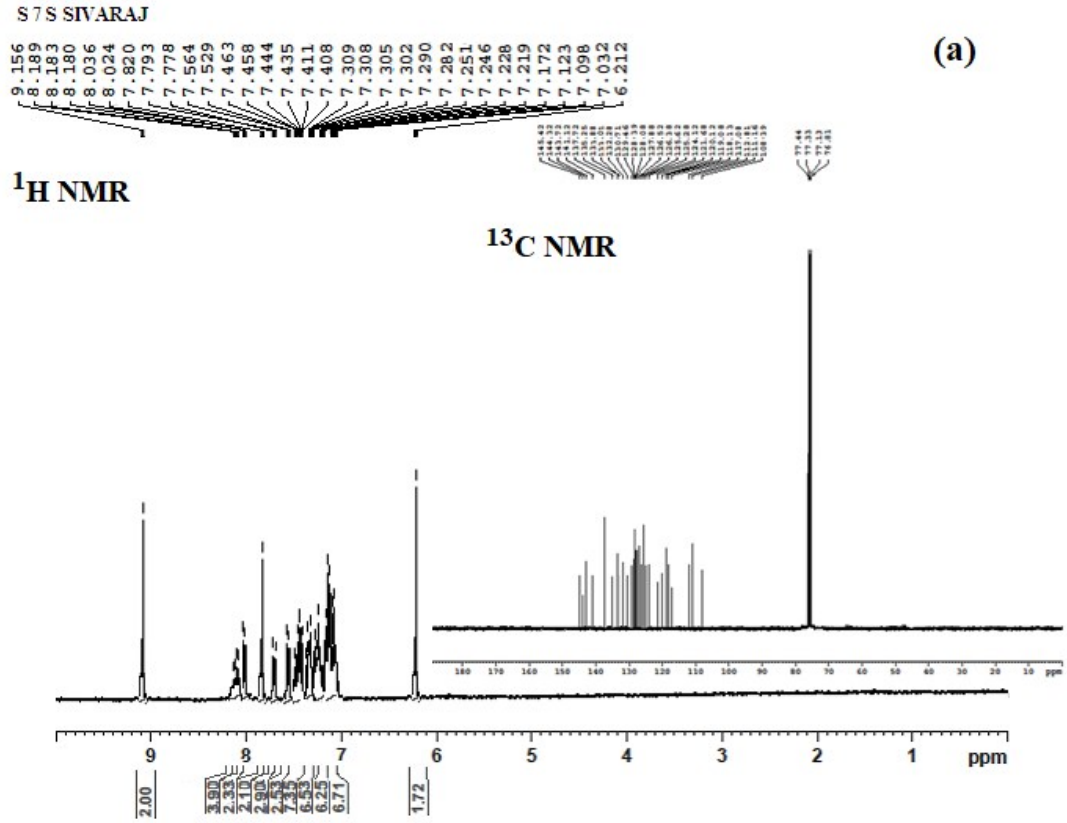

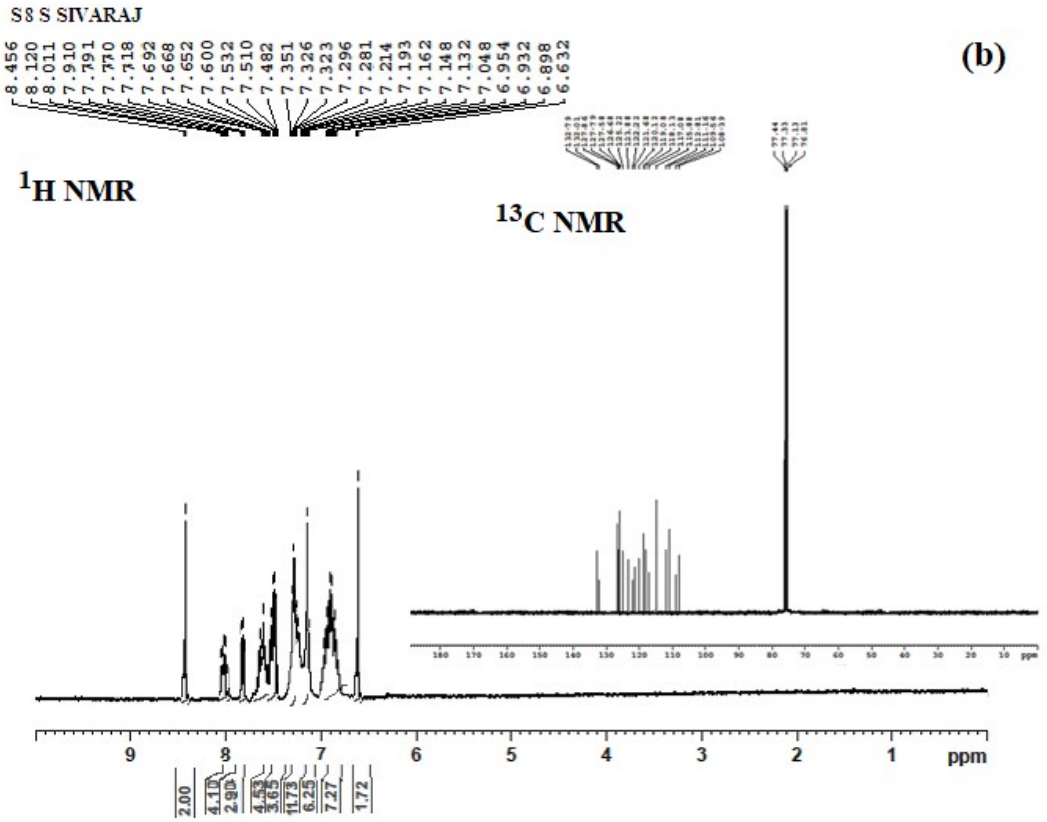

Scheme S3. Spectra of (a)**PPI-Py**; (b) **PPICN-Py**

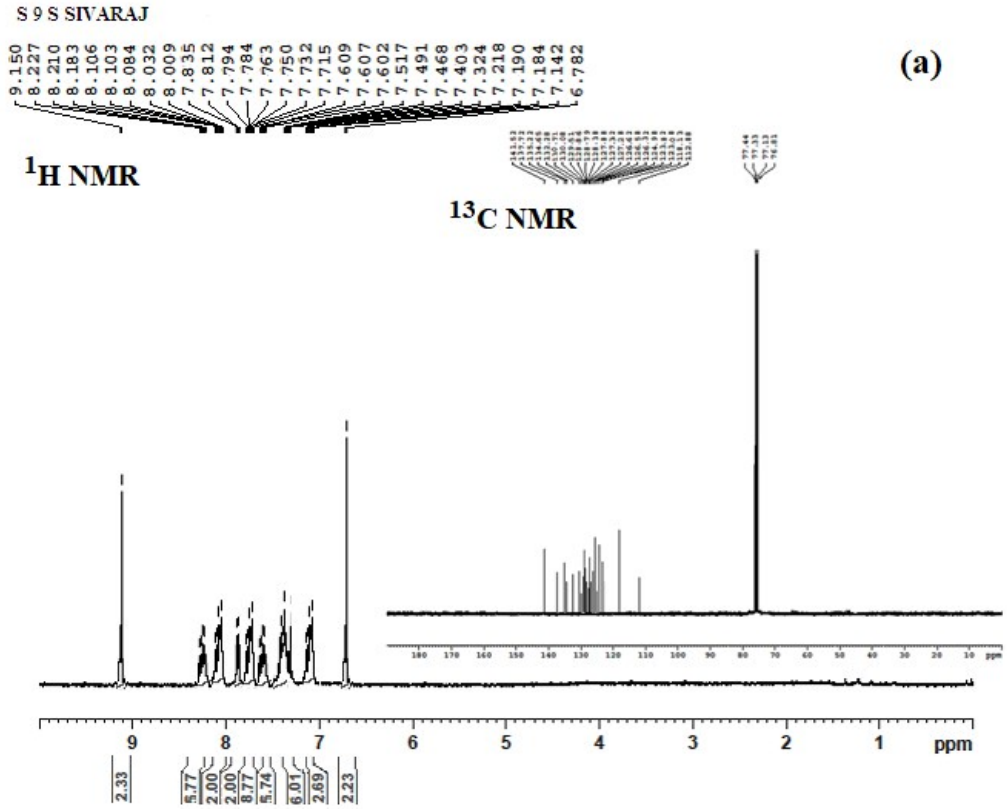

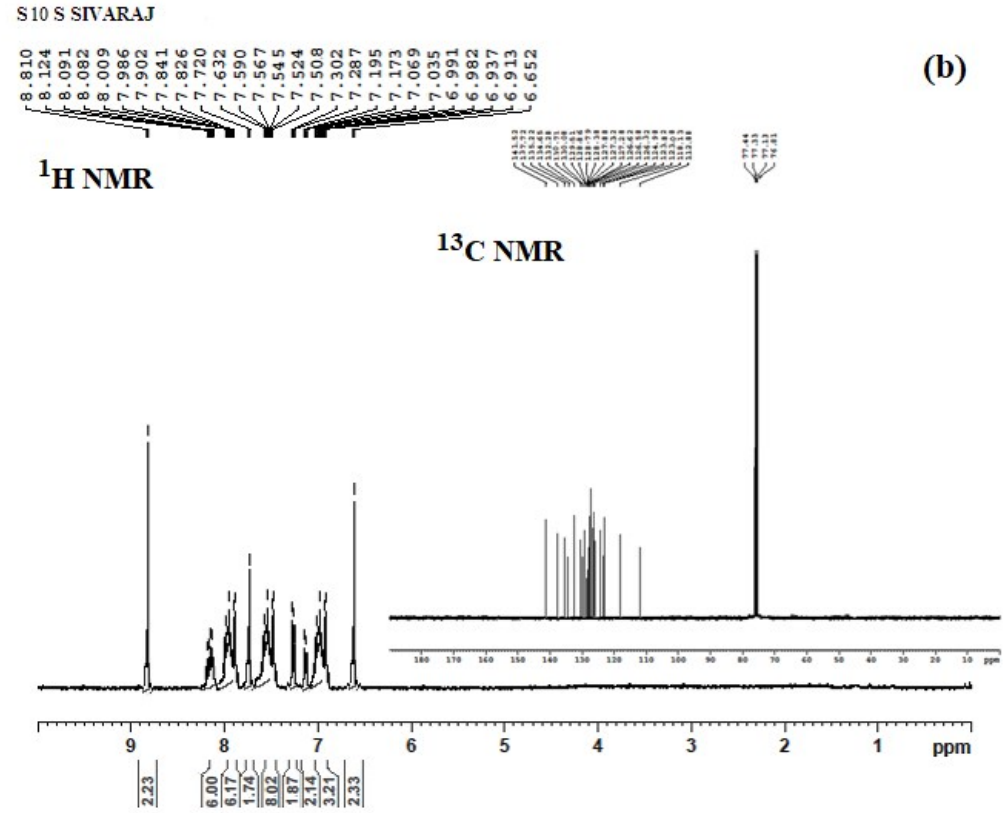

Scheme S4. Spectra of (a)PPI-An; (b) PPICN-An

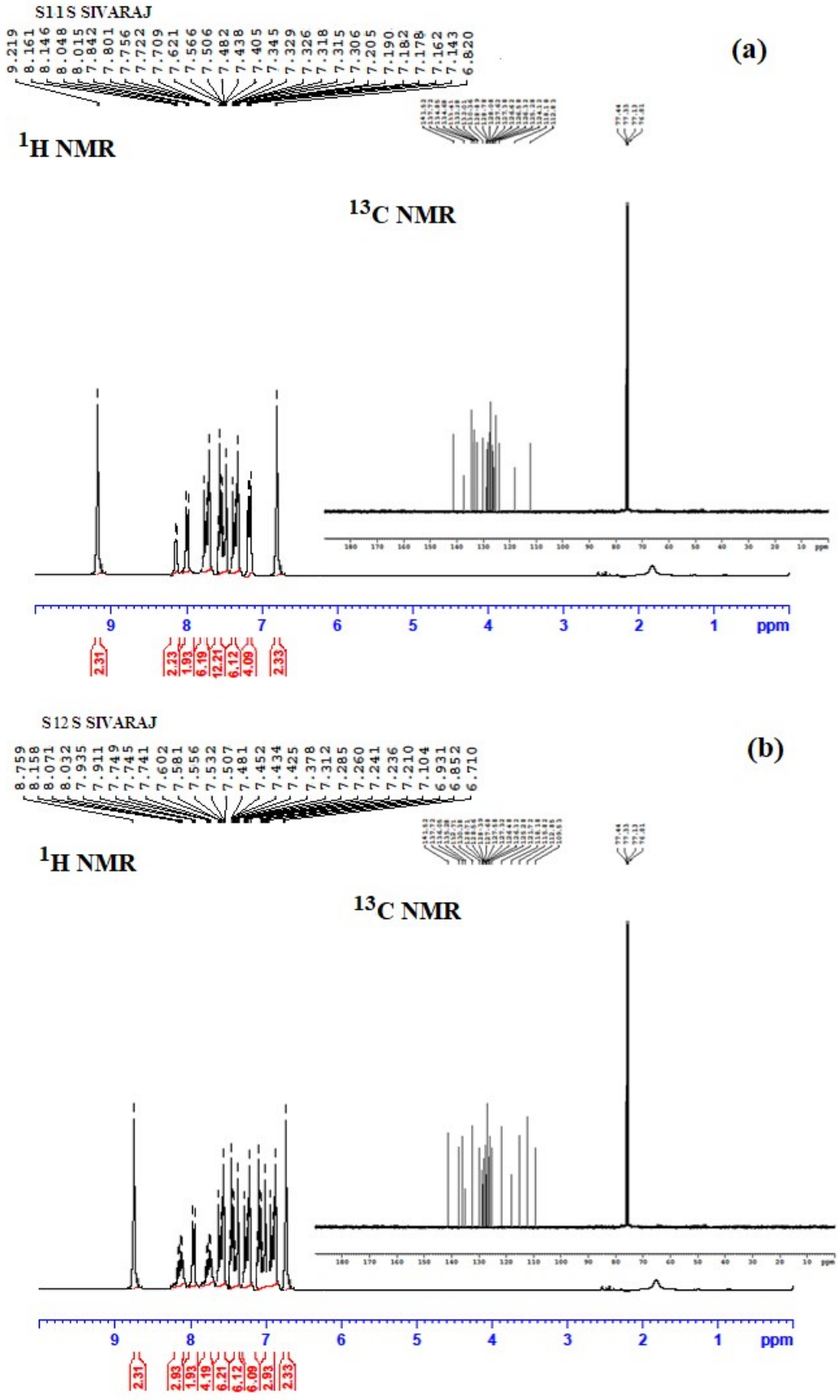

Scheme S5. Spectra of (a)PPI-Cz; (b) PPICN-Cz; (c)PPI-Py; (d) PPICN-Py; (e)PPI-An; (f) PPICN-An.

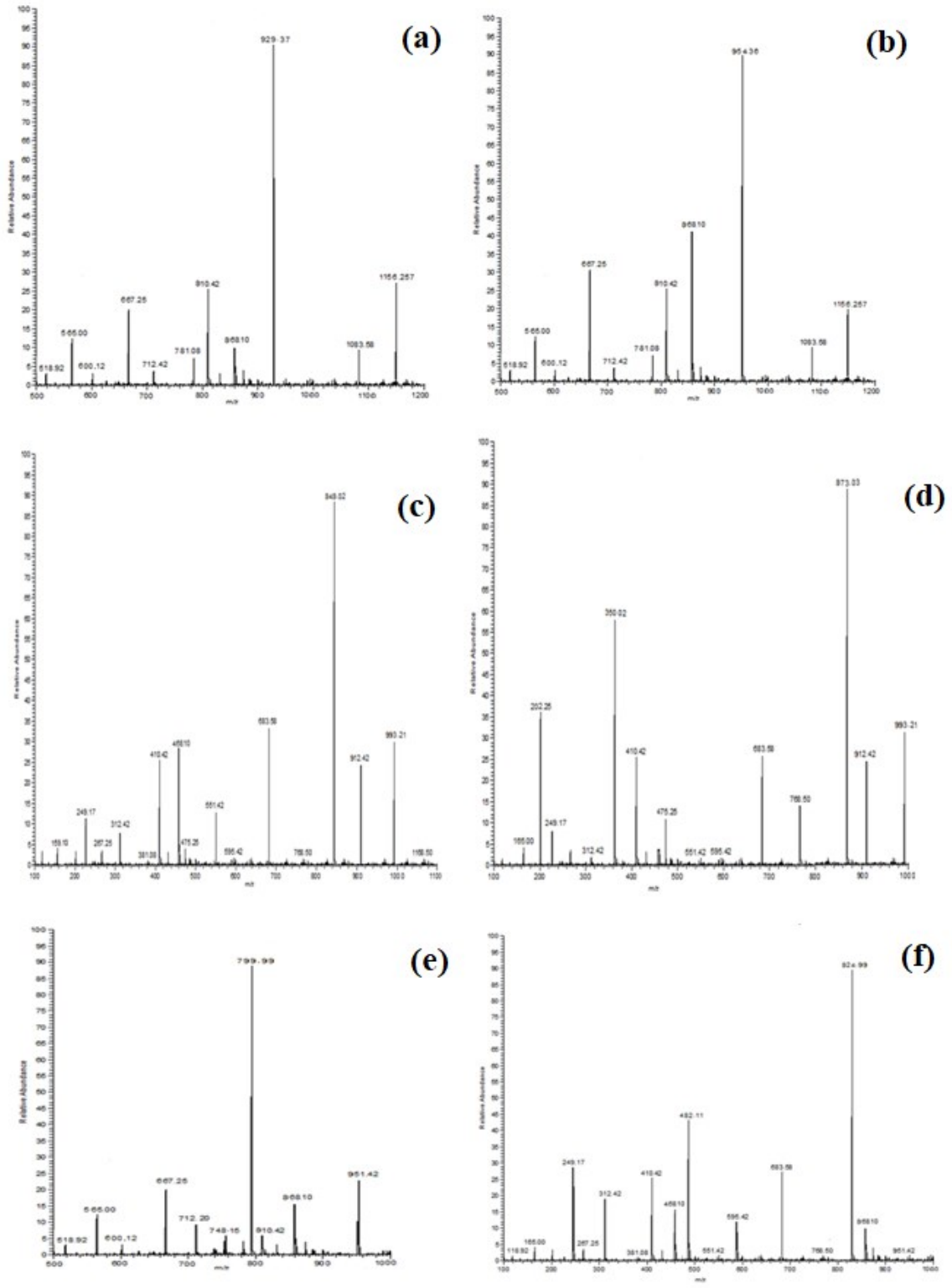

SI-III: Figure S1 (a) AFM images; (b) Favoured and unfavoured configurations of blue emitters

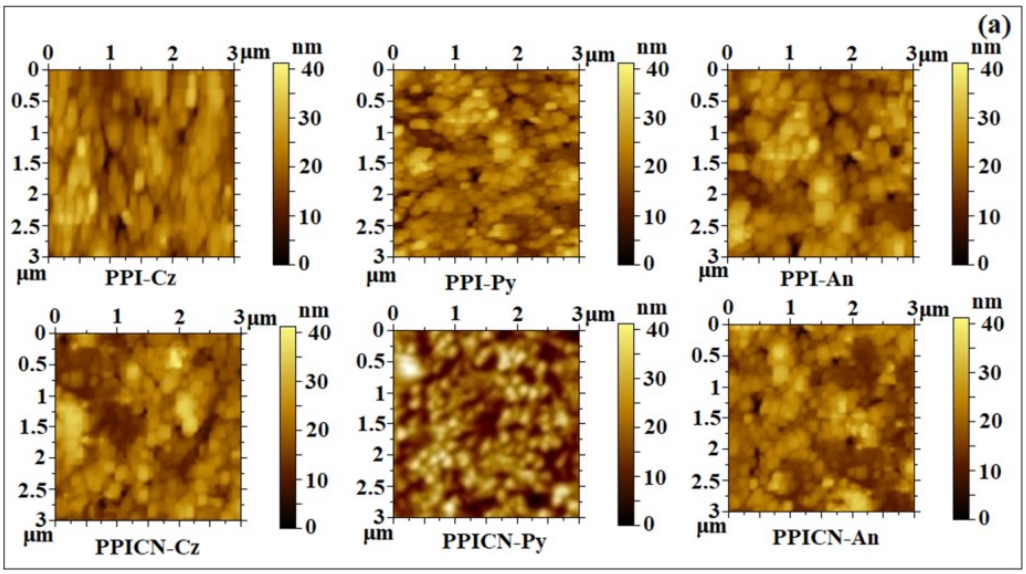

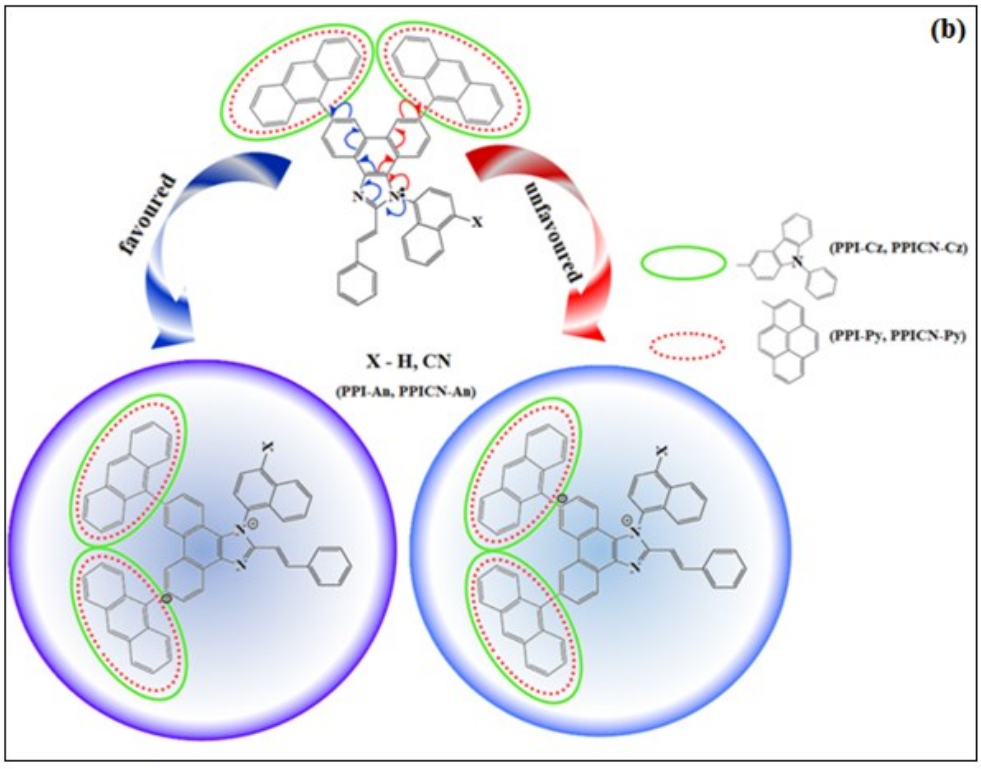

SI-IV: Solvatochromism (Figures S2-S4):

Figure S2. Absorption spectra of emissive materials.

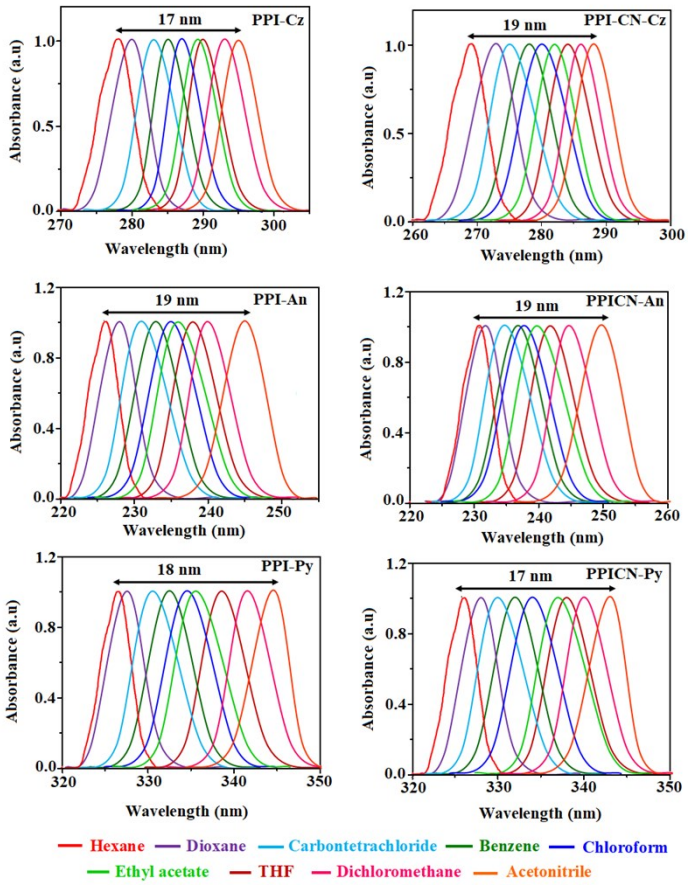

Figure S3. Emission spectra of emissive materials.

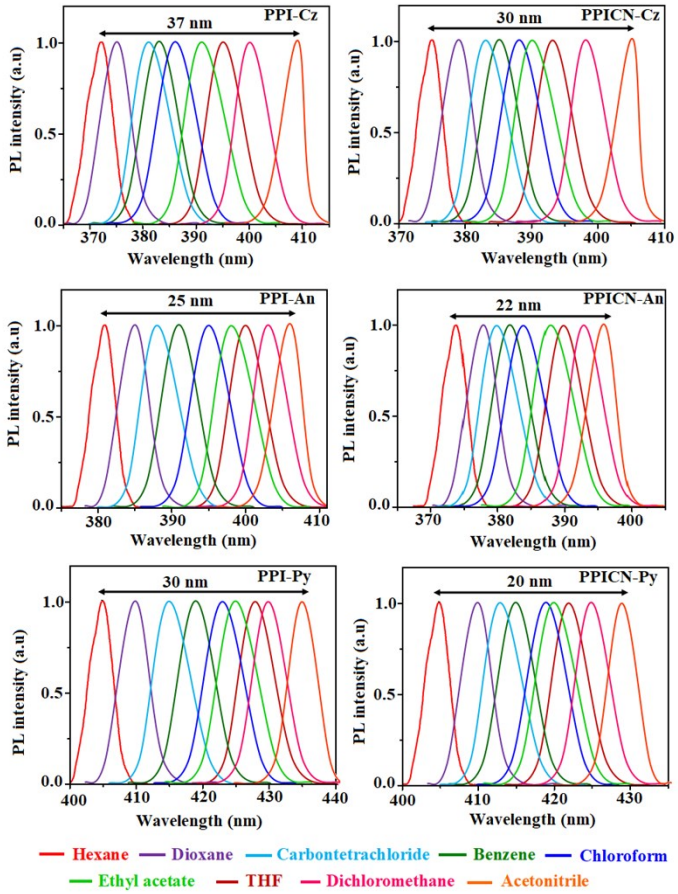

SI-V: Figure S4. Lippert - Mataga plot.

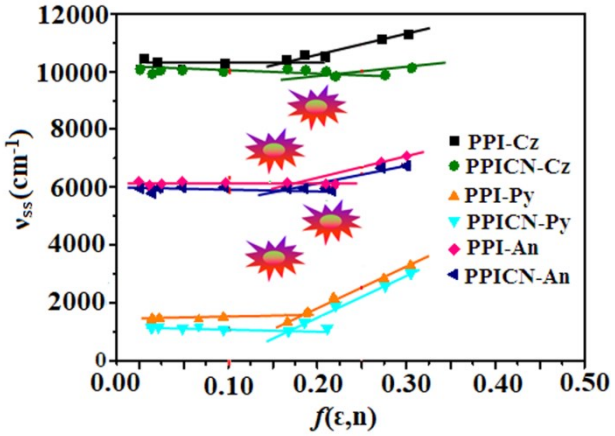

SI–V: Charge-Transfer Intexes

The hole-particle pair interactions have been related to the distance covered during the excitations one possible descriptor Δr index could be used to calculate the average distance which is weighted in function of the excitation coefficients.

$$\Delta r = \frac{\Sigma_{ia} k_{ia}^2 \left| \langle \varphi_a | r | \varphi_a \rangle - \langle \varphi_i | r | \varphi_i \rangle \right|}{\Sigma_{ia} K_{ia}^2} \quad \text{..... (S1)}$$

Where $\left| \langle \varphi_i | r | \varphi_i \rangle \right|$ is the norm of the orbital centroid [1–4] and Δr index will be expressed in Å. The density variation associated to the electronic transition is given by

$$\Delta\rho(r) = \rho_{EX}(r) - \rho_{GS}(r) \quad \text{..... (S2)}$$

Where $\rho_{GS}(r)$ and $\rho_{EX}(r)$ are the electronic densities of to the ground and excited states, respectively. Two functions, $\rho_+(r)$ and $\rho_-(r)$, corresponds to the points in space where an increment or a depletion of the density upon absorption is produced and they can be defined as follows:

$$\rho_+(r) = \begin{Bmatrix} \Delta\rho(r) if \Delta\rho(r) > 0 \\ 0 \quad if \Delta\rho(r) < 0 \end{Bmatrix} \quad \text{..... (S3)}$$

$$\rho_-(r) = \begin{Bmatrix} \Delta\rho(r) if \Delta\rho(r) < 0 \\ 0 \quad if \Delta\rho(r) > 0 \end{Bmatrix} \quad \text{..... (S4)}$$

The barycenters of the spatial regions R_+ and R_- are related with $\rho_+(r)$ and $\rho_-(r)$ and are shown as

$$R_+ = \frac{\int r\rho_+(r)dr}{\int \rho_+(r)dr} = (x_+, y_+, z_+) \quad \text{..... (S5)}$$

$$R_- = \frac{\int r\rho_-(r)dr}{\int \rho_-(r)dr} = (x_-, y_-, z_-) \quad \text{..... (S6)}$$

The spatial distance (D_{CT}) between the two barycenters R_+ and R_- of density distributions can thus be used to measure the CT excitation length

$$D_{CT} = |R_+ - R_-| \quad \text{..... (S7)}$$

The transferred charge (q_{CT}) can be obtained by integrating over all space $\rho_+(\rho_-)$,. Variation in dipole moment between the ground and the excited states (μ_{CT}) can be computed by the following relation:

$$\|\mu_{CT}\| = D_{CT}\int \rho_+(r)dr = D_{CT}\int \rho_-(r)dr \quad \text{..... (S8)}$$

$$= D_{CT}q_{CT} \quad \text{..... (S9)}$$

The difference between the dipole moments $\|\mu_{CT}\|$ have been computed for the ground and the excited states $\Delta\mu_{ES-GS}$. The two centroids of charges (C^+/C^-) associated to the positive and negative density regions are calculated as follows. First the root-mean-square deviations along the three axis (σ_{aj}, j = x, y, z; a = + or –) are computed as

$$\sigma_{a,j} = \sqrt{\frac{\sum_i \rho_a(r_i)(j_i - j_a)^2}{\sum_i \rho_a(r_i)}} \quad \text{..... (S10)}$$

The two centroids (C_+ and C_-) are defined as

$$C_+(r) = A_+ e\left(-\frac{(x-x_+)^2}{2\sigma_{+x}^2} - \frac{(y-y_+)^2}{2\sigma_{+y}^2} - \frac{(z-z_+)^2}{2\sigma_{+z}^2}\right) \quad \text{..... (S11)}$$

$$C_-(r) = A_- e\left(-\frac{(x-x_-)^2}{2\sigma_{-x}^2} - \frac{(y-y_-)^2}{2\sigma_{-y}^2} - \frac{(z-z_-)^2}{2\sigma_{-z}^2}\right) \quad \text{..... (S12)}$$

The normalization factors (A+ and A_) are used to impose the integrated charge on the centroid to be equal to the corresponding density change integrated in the whole space:

$$A_{+} = \frac{\int \rho_{+}(r)dr}{\int e\left(-\frac{(x-x_{-})^2}{2\sigma_{+x}^2} - \frac{(y-y_{-})^2}{2\sigma_{+y}^2} - \frac{(z-z_{-})^2}{2\sigma_{+z}^2}\right)dr} \quad \text{..... (S13)}$$

$$A_{-} = \frac{\int \rho_{-}(r)dr}{\int e\left(-\frac{(x-x_{-})^2}{2\sigma_{-x}^2} - \frac{(y-y_{-})^2}{2\sigma_{-y}^2} - \frac{(z-z_{-})^2}{2\sigma_{-z}^2}\right)dr} \quad \text{..... (S14)}$$

H index is defined as half of the sum of the centroids axis along the D–A direction, if the D–A direction is along the X axis, H is defined by the relation:

$$H = \frac{\sigma_{+x} + \sigma_{-x}}{2} \quad \text{..... (S15)}$$

The centroid along X axis is expected. The t index represents the difference between D_{CT} and H:

$$t = D_{CT} - H \quad \text{..... (S16)}$$

SI-VI: Natural Transition Orbitals (NTOs)

The excited-state properties were examined to gain a deep insight into the intrinsic photophysics of these materials. Both natural transition orbital (NTO) and electron-hole pair wavefunction were used to describe the excited state character. The HONTOs and LUNTOs of PPI-Cz, PPICN-Cz, PPI-An, PPICN-An, PPI-Py and PPICN-Py (Figures S5-S7: Tables S7- S9) exhibit a hybrid splitting state character from interstate coupling of LE and CT levels. The % CT increases as increasing the aromatic fragment size and also partially influenced by steric hindrance. The increasing % LE in S_1 state enhances the photoluminance efficiency (η_{PL}).

Thus, compared with N-phenylcarbazole and anthracene substituted phenanthrimidazole, PPI-Py and PPICN-Py exhibits high photoluminance efficiency (η_{PL}), high exciton utilisation efficiency (η_S) and high external quantum efficiency (η_{EQE}) as a result of increased LE component in S_1 state.

Figure S5. Natural transition orbital pairs (HONTOs and LUNTOs) with transition character analysis of PPI-Cz and PPICN-Cz.

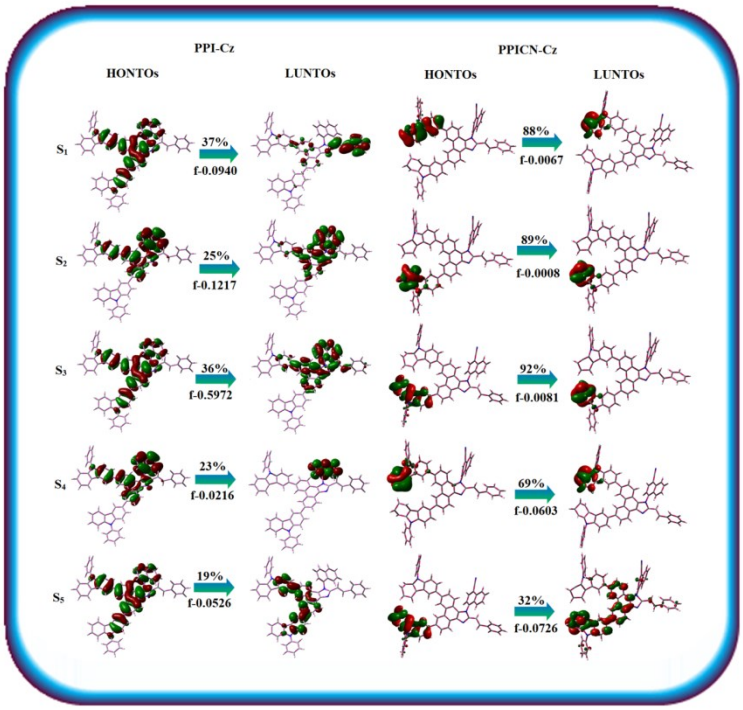

Figure S6. Natural transition orbital pairs (HONTOs and LUNTOs) with transition character analysis of PPI-An and PPICN-An.

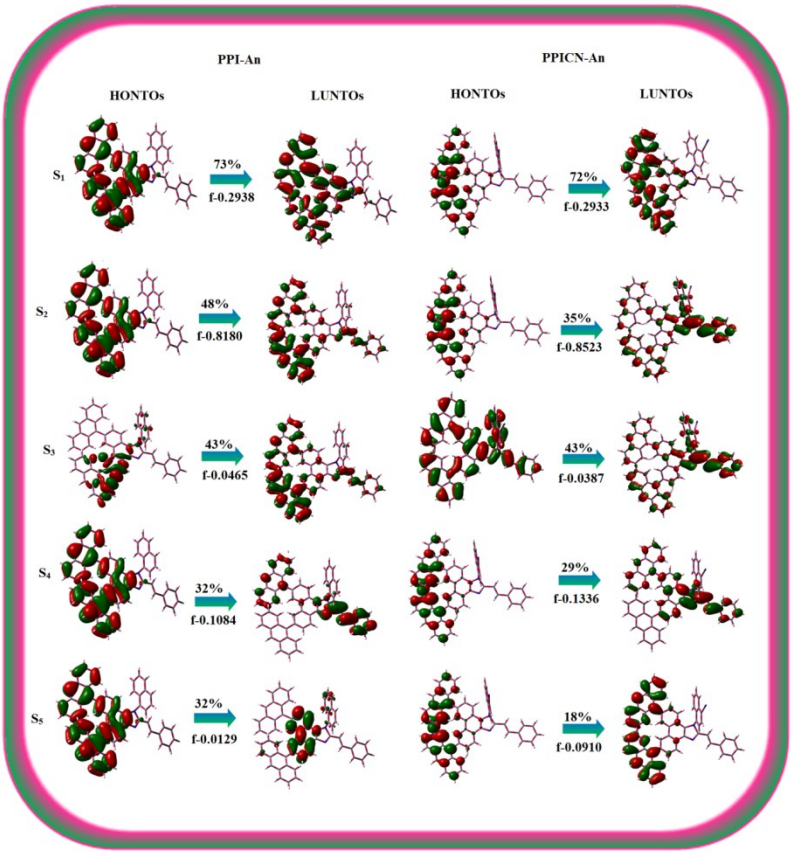
PPI-An
PPICN-An
HONTOs
LUNTOs
HONTOs
LUNTOs
S1
73%
f-0.2938
72%
f-0.2933
S2
48%
f-0.8180
35%
f-0.8523
S3
43%
f-0.0465
43%
f-0.0387
S4
32%
f-0.1084
29%
f-0.1336
S5
32%
f-0.0129
18%
f-0.0910

Figure S7. Natural transition orbital pairs (HONTOs and LUNTOs) with transition character analysis for singlet states of PPI-Py and PPICN-Py.

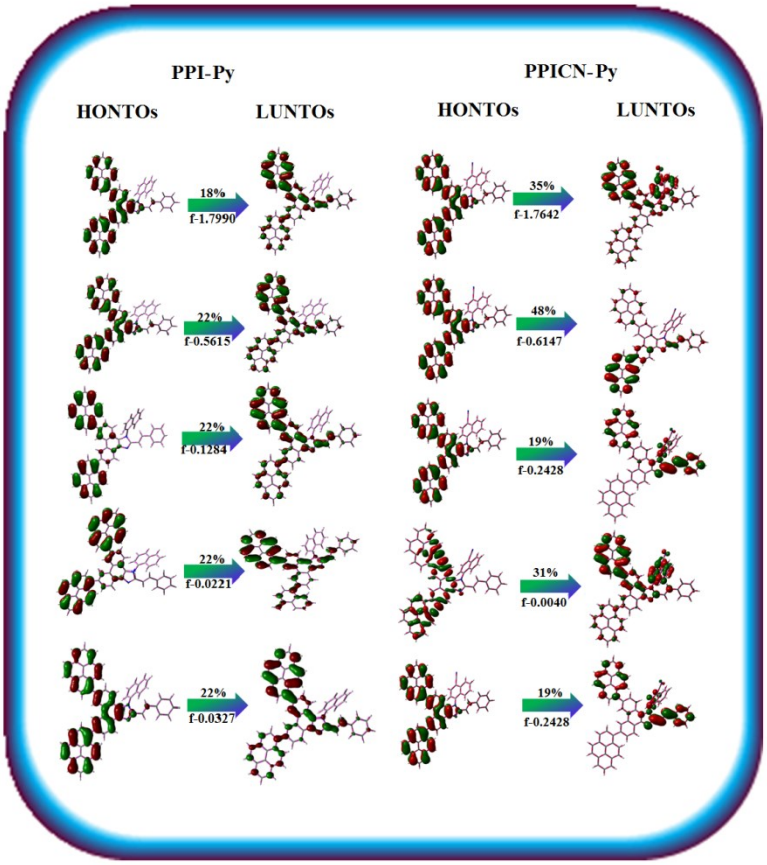

SI-VII: Hole-Particle Distribution

The integral of hole (h^+) and electron (e^-) of these materials with transition density is shown in Figures S8-S10. The integral overlap of hole-electron (Tables S10-S15) distribution (S) is a measure of spatial separation of hole and electron. The integral overlap (S) of hole and electron and distance (D) between centroids of hole and electron confirmed the existence of LE and CT states. Compared to parent compounds, these emitters has small D and high S value, however, The small D and high S of cyano phenanthroimidazoles on comparison to parent indicates charge transfer is higher in percentage in cyano phenanthroimidazoles. The variation of dipolemoment with respect to S_0 is outputted which is directly evaluated based on the position of centroid of hole and electron. RMSD of hole or electron characterizes their distribution breadth:

RMSD of both electron and hole in PPI-Py/ PPICN-Py and PPI-Cz/ PPICN-Cz is higher in X direction, indicates electron and hole distribution is much broader in X direction whereas RMSD of electron in PPI-An/ PPICN-Anis higher in Y direction, indicates electron and hole distribution is much broader in Y direction. The H index (half sum of the axis of anistropic density variation distribution) measures the spread of positive and negative regions related to CT. The CT index, *i.e., t* index is another measure of separation of hole-electron (equations S15 and S16; Tables S10-S12). For both CADPPI and TPNCN-TPA, *t* is negative in all directions which reveal that the overlap of hole and electron is severe (Figure S8). This is further evidenced by Δr index (equation S1) which is average of hole -electron distance ($d_{h^+ - e^-}$) upon excitation which shows the nature of excitation type, LE or CT: valence excitation (LE) is related to short distance (< $d_{h^+ - e^-}$) while the larger distance (> $d_{h^+ - e^-}$) is related to CT excitation.

Figure S8. Hole and particle distribution of PPI-Cz and PPICN-Cz.

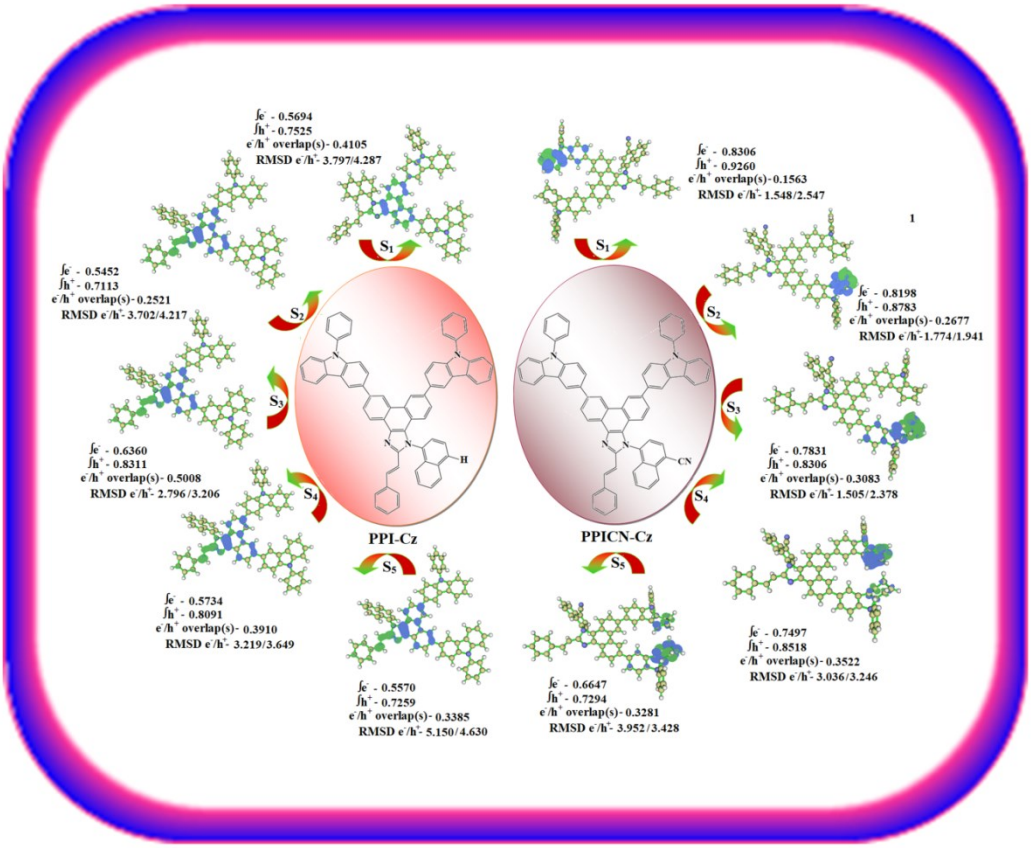

Figure S9. Hole and particle distribution of PPI-An and PPICN-An

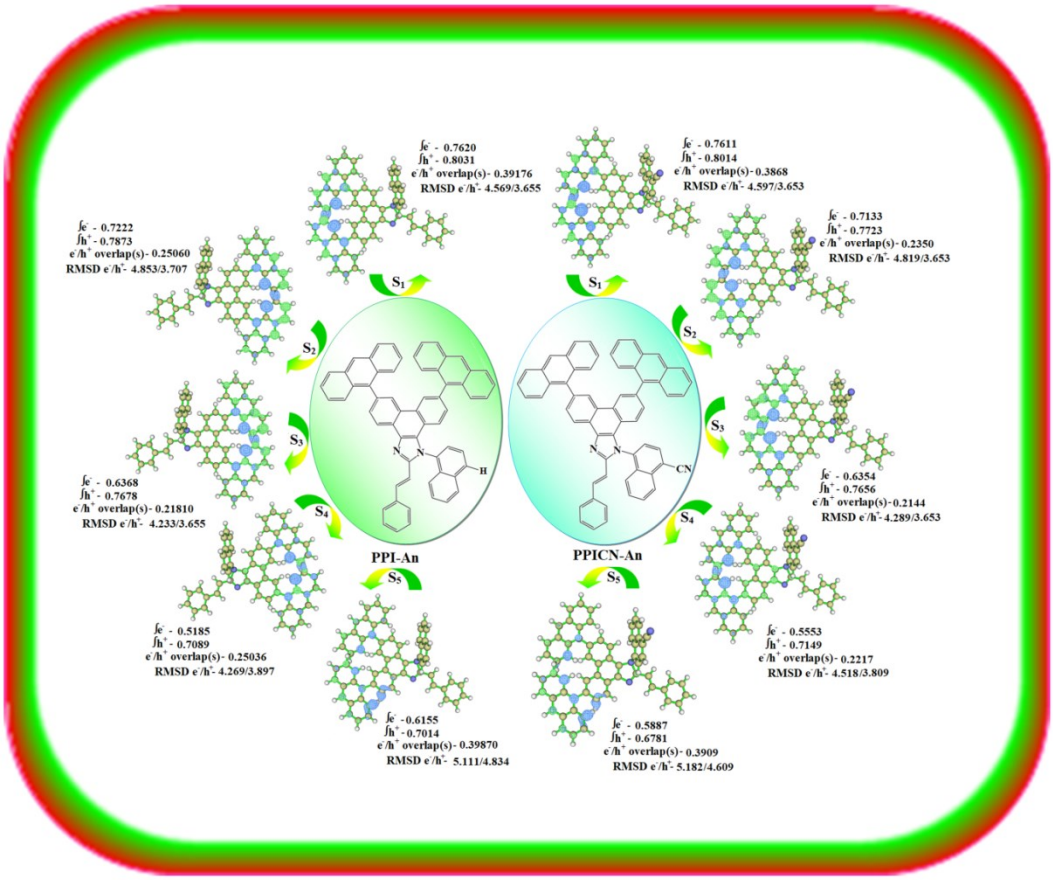

Figure S10. Hole and particle distribution of PPI-Py and PPICN-Py

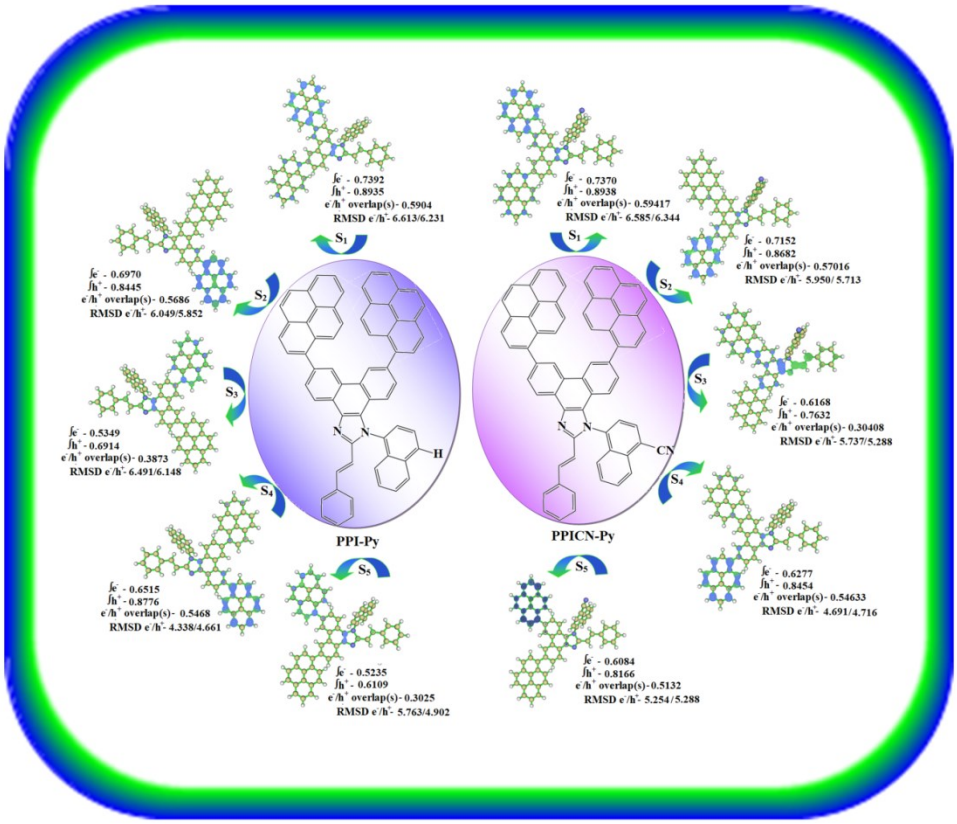

SI-VIII: Potential Energy Scan (PES)

The potential energy surfaces (PES) have been plotted as a function of twist angle between C2 substituent and phenanthrimidazole core in gas phase (Figure S11). During calculation all geometrical parameters were simultaneously relaxed while torsional angles were varied in steps of 0˚, 20˚, 40˚, 60˚….360˚. Tuning the substituent at C6/C9 positions have small influence on twist angles between phenanthrimidazole plane and naphthyl group and much larger variation in θ3 and θ4 angle (θ_1-PPI and C-coupling; θ_2-PPI and N-coupling; θ3-C6 and PPI; θ4-C9 and PPI-N-coupling). The synthesized emitters show more twisted configuration (θ_1~25°; θ_2~75°; θ_3~55°; θ_4~56.0°) due to larger steric hindrance between the substituent with phenanthrimidazole core. The non-coplanar twisted conformation can effectively suppress the molecular aggregation, the almost orthogonal dihedral angles (~89.0°) between N-coupling and phenanthrimidazole core effectively minimize the intermolecular packing and used as hole-trapping sites whereas peripheral phenanthrimidazole core blocks electron-trapping sites. Thus, effective carrier injection as well as transport ability will be expected from these reported emitter and the relative charge carrier transport ability of the title materials was investigated by hole-only devices as well as electron-only devices. The introduction of C6/C9 substituents on phenanthroimidazole unit could enhance the molecular distortion degree, thereby suppress the formation of aggregation or π-π stacking in the solid state and form amorphous film during device fabrication The non-planar conformation may effectively suppresses red shift and maintains quantum efficiency in film *via* restraining intermolecular interaction. The incorporation of bulky fragments at C6/C9 positions and side capping into phenanthroimidazoles enlarged the size and improved their thermal stability.

Figure S11. Potential energy surface scan (PES) diagram of emissive materials.

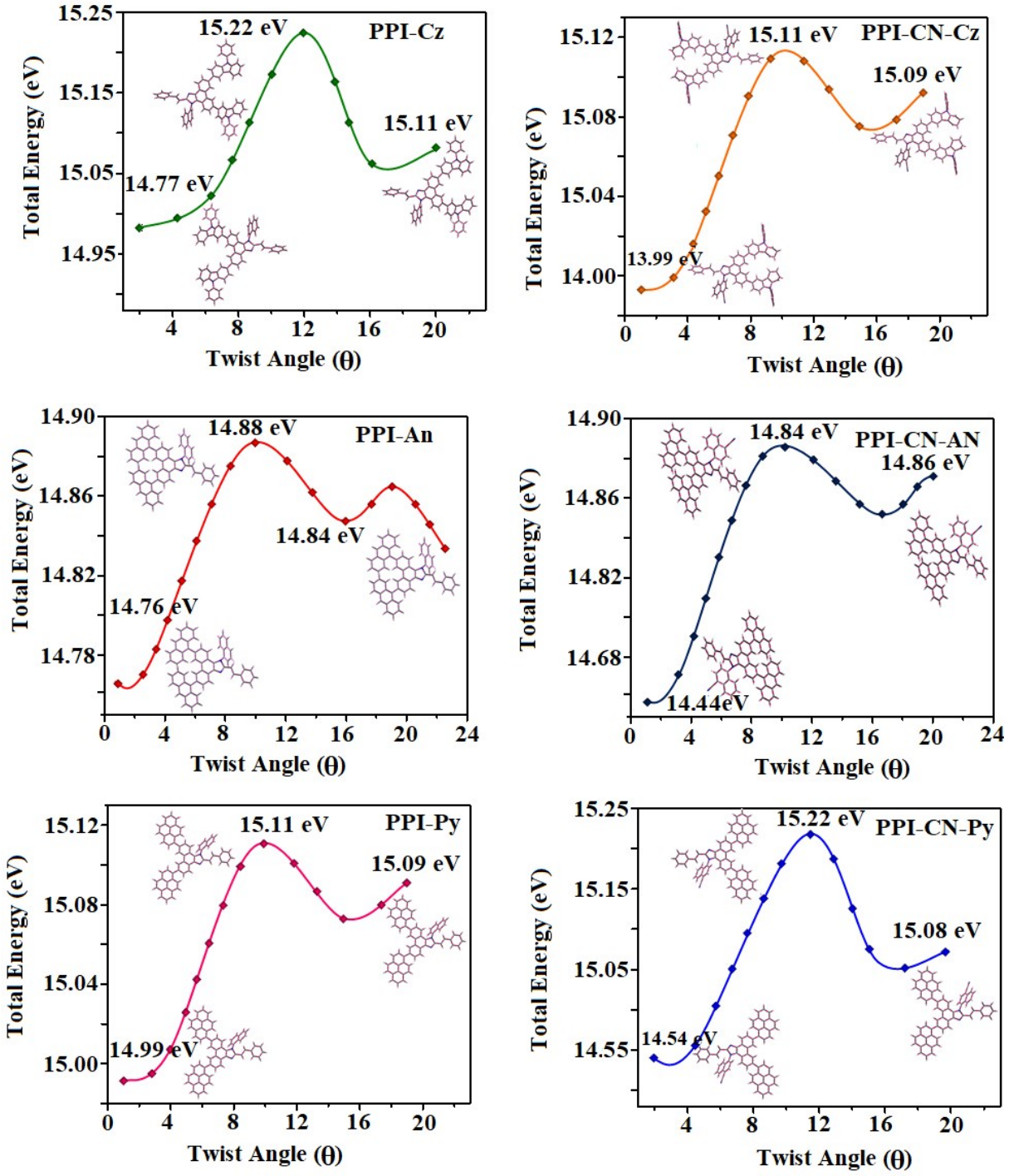

SI-IX: Tables S1-S15

Table S1: Photophysical properties of PPI-Cz in different solvents.

Solvents	**ε**	**n**	**f(ε,n)**	**λ_{ab} (nm)**	**ν_{ab} (cm^{-1})**	**λ_{flu} (nm)**	**ν_{flu} (cm^{-1})**	**ν_{ss} (cm^{-1})**	**ΔG (kcal/mol)**	**$\Delta(\Delta G_{hex}-\Delta G_{sol})$ (kcal/mol)**	**λ (kcal/mol)**
hexane	2.42	1.401	0.048	278	34482.76	372	24271.84	10210.91	83.98	8.15	14.59
dioxane	3.39	1.474	0.0878	280	34246.58	375	24038.46	10653.57	83.55	8.03	14.66
CCl_4	3.08	1.399	0.096	283	34364.26	381	24271.84	10092.42	83.81	8.32	14.42
benzene	4.33	1.352	0.1669	285	34602.08	383	24271.84	10330.23	84.15	7.98	14.76
chloroform	6.09	1.4131	0.186569	287	34602.08	386	24038.46	10563.61	83.81	8.31	15.10
ethyl acetate	7.52	1.405	0.209634	289	34364.26	391	23980.82	10383.45	83.39	8.73	14.84
THF	9.08	1.4242	0.218349	290	34129.69	395	25000	9129.693	84.51	7.61	13.05
dichloromethane	36.7	1.427	0.276	293	34722.22	400	25062.66	9659.566	85.45	6.67	13.80
acetonitrile	37.5	1.3442	0.305378	295	34364.26	40	24330.9	10033.36	83.89	8.23	14.34

Table S2: Photophysical properties of PPI-CN-Cz in different solvents.

Solvents	**ε**	**n**	**f(ε,n)**	**ET(30)**	**λ_{ab} (nm)**	**ν_{ab} (cm^{-1})**	**λ_{flu} (nm)**	**ν_{flu} (cm^{-1})**	**ν_{ss} (cm^{-1})**	**ΔG (kcal/mol)**	**$\Delta(\Delta G_{hex}-\Delta G_{sol})$ (kcal/mol)**	**λ (kcal/mol)**
hexane	1.88	1.37	0.000411	32.4	269	44052.86	375	24752.48	19300.39	98.34	-15.82	27.59
dioxane	2.22	1.42	0.021437	36.0	273	43103.45	379	24449.88	18653.57	96.55	-14.03	26.66
CCl_4	2.23	1.46	0.011075	39.1	275	41841.00	383	24038.46	17802.54	94.16	-11.64	25.44
benzene	2.28	1.42	0.026639	34.3	278	41152.26	385	23696.68	17455.58	92.69	-10.17	24.95
chloroform	4.81	1.44	0.148262	39.1	280	40322.58	388	23041.47	17281.11	90.56	-8.04	24.70
ethyl acetate	6.09	1.41	0.186569	38.1	282	40000.00	390	22573.36	17426.64	89.43	-6.91	24.91
THF	7.52	1.40	0.209634	37.4	284	39062.50	393	22026.43	17036.07	87.31	-4.79	24.35
dichloromethane	9.08	1.42	0.218349	40.7	286	40322.58	398	21739.13	18583.45	88.70	-6.18	26.56
acetonitrile	37.5	1.34	0.305378	45.6	288	38759.69	405	21459.23	17300.46	86.07	-3.55	24.73

Table S3: Photophysical properties of PPI- An in different solvents.

Solvents	**ε**	**n**	**f(ε,n)**	**ET(30)**	**λ_{ab} (nm)**	**ν_{ab} (cm^{-1})**	**λ_{flu} (nm)**	**ν_{flu} (cm^{-1})**	**ν_{ss} (cm^{-1})**	**ΔG (kcal/mol)**	**$\Delta(\Delta G_{hex}-\Delta G_{sol})$ (kcal/mol)**	**λ (kcal/mol)**
hexane	1.88	1.37	0.000411	32.4	226	43103.45	381	24330.9	18772.55	96.38	-13.86	26.83
dioxane	2.22	1.42	0.021437	36.0	228	42194.09	385	24038.46	18155.63	94.66	-12.14	25.95
CCl_4	2.23	1.46	0.011075	39.1	231	41322.31	388	23752.97	17569.34	93.01	-10.49	25.11
benzene	2.28	1.42	0.026639	34.3	233	41152.26	391	23364.49	17787.78	92.21	-9.69	25.42
chloroform	4.81	1.44	0.148262	39.1	235	40485.83	395	22988.51	17497.32	90.72	-8.20	25.01
ethyl acetate	6.09	1.41	0.186569	38.1	236	40160.64	398	22727.27	17433.37	89.88	-7.36	24.92
THF	7.52	1.40	0.209634	37.4	238	40000.00	400	22421.52	17578.48	89.22	-6.70	25.12
dichloromethane	9.08	1.42	0.218349	40.7	240	40322.58	403	21739.13	18583.45	88.70	-6.18	26.56
acetonitrile	37.5	1.34	0.305378	45.6	245	39062.5	406	22172.95	16889.55	87.52	-5.00	24.14

Table S4: Photophysical properties of PPI- CN-An in different solvents.

Solvents	**ε**	**n**	**f(ε,n)**	**ET(30)**	**λ_{ab} (nm)**	**ν_{ab} (cm^{-1})**	**λ_{flu} (nm)**	**ν_{flu} (cm^{-1})**	**ν_{ss} (cm^{-1})**	**ΔG (kcal/mol)**	**$\Delta(\Delta G_{hex}-\Delta G_{sol})$ (kcal/mol)**	**λ (kcal/mol)**
hexane	1.88	1.37	0.000411	32.4	231	44052.86	374	24752.48	19300.39	98.34	-15.82	27.59
dioxane	2.22	1.42	0.021437	36.0	232	43103.45	378	24449.88	18653.57	96.55	-14.03	26.66
CCl_4	2.23	1.46	0.011075	39.1	235	41841.00	380	24038.46	17802.54	94.16	-11.64	25.44
benzene	2.28	1.42	0.026639	34.3	237	41152.26	382	23696.68	17455.58	92.69	-10.17	24.95
chloroform	4.81	1.44	0.148262	39.1	238	40322.58	384	23041.47	17281.11	90.56	-8.04	24.70
ethyl acetate	6.09	1.41	0.186569	38.1	240	40000.00	388	22573.36	17426.64	89.43	-6.91	24.91
THF	7.52	1.40	0.209634	37.4	242	39062.50	390	22026.43	17036.07	87.31	-4.79	24.35
dichloromethane	9.08	1.42	0.218349	40.7	245	40322.58	393	21739.13	18583.45	88.70	-6.18	26.56
acetonitrile	37.5	1.34	0.305378	45.6	250	38759.69	396	21459.23	17300.46	86.07	-3.55	24.73

Table S5: Photophysical properties of PPI- Py in different solvents.

Solvents	**ε**	**n**	**f(ε,n)**	**ET(30)**	**λ_{ab} (nm)**	**ν_{ab} (cm^{-1})**	**λ_{flu} (nm)**	**ν_{flu} (cm^{-1})**	**ν_{ss} (cm^{-1})**	**ΔG (kcal/mol)**	**$\Delta(\Delta G_{hex}-\Delta G_{sol})$ (kcal/mol)**	**λ (kcal/mol)**
hexane	1.88	1.37	0.000411	32.4	327	43103.45	405	24330.9	18772.55	96.38	-13.86	26.83
dioxane	2.22	1.42	0.021437	36.0	328	42194.09	410	24038.46	18155.63	94.66	-12.14	25.95
CCl_4	2.23	1.46	0.011075	39.1	331	41322.31	415	23752.97	17569.34	93.01	-10.49	25.11
benzene	2.28	1.42	0.026639	34.3	333	41152.26	419	23364.49	17787.78	92.21	-9.69	25.42
chloroform	4.81	1.44	0.148262	39.1	335	40485.83	423	22988.51	17497.32	90.72	-8.20	25.01
ethyl acetate	6.09	1.41	0.186569	38.1	336	40160.64	425	22727.27	17433.37	89.88	-7.36	24.92
THF	7.52	1.40	0.209634	37.4	339	40000	428	22421.52	17578.48	89.22	-6.70	25.12
dichloromethane	9.08	1.42	0.218349	40.7	342	40322.58	430	21739.13	18583.45	88.70	-6.18	26.56
acetonitrile	37.5	1.34	0.305378	45.6	345	39062.5	435	22172.95	16889.55	87.52	-5.00	24.14

Table S6: Photophysical properties of PPI- CN-Py in different solvents.

Solvents	**ε**	**n**	**f(ε,n)**	**ET(30)**	**λ_{ab} (nm)**	**ν_{ab} (cm^{-1})**	**λ_{flu} (nm)**	**ν_{flu} (cm^{-1})**	**ν_{ss} (cm^{-1})**	**ΔG (kcal/mol)**	**$\Delta(\Delta G_{hex}-\Delta G_{sol})$ (kcal/mol)**	**λ (kcal/mol)**
hexane	1.88	1.37	0.000411	32.4	326	44052.86	405	24752.48	19300.39	98.34	-15.82	27.59
dioxane	2.22	1.42	0.021437	36.0	328	43103.45	410	24449.88	18653.57	96.55	-14.03	26.66
CCl_4	2.23	1.46	0.011075	39.1	330	41841.00	413	24038.46	17802.54	94.16	-11.64	25.44
benzene	2.28	1.42	0.026639	34.3	332	41152.26	415	23696.68	17455.58	92.69	-10.17	24.95
chloroform	4.81	1.44	0.148262	39.1	334	40322.58	419	23041.47	17281.11	90.56	-8.04	24.70
ethyl acetate	6.09	1.41	0.186569	38.1	337	40000.00	420	22573.36	17426.64	89.43	-6.91	24.91
THF	7.52	1.40	0.209634	37.4	338	39062.50	422	22026.43	17036.07	87.31	-4.79	24.35
dichloromethane	9.08	1.42	0.218349	40.7	340	40322.58	425	21739.13	18583.45	88.70	-6.18	26.56
acetonitrile	37.5	1.34	0.305378	45.6	343	38759.69	429	21459.23	17300.46	86.07	-3.55	24.73

Table S7: Computed excitation energy (eV), excitation coefficient, Δr (Å), oscillator strength (*f*) and dipolemoment (μ, D) for singlet states of PPI-Cz and PPICN-Cz.

Emitters	State	Excitation energy	Excitation coefficient	Δr	Oscillator strength	μ	NTO Transitions
PPI-Cz	1	3.44	0.3599	2.5807	0.0940	0.80	$170 \xrightarrow{37\%} 174$
	2	3.50	0.3496	2.0300	0.1217	0.52	$169 \xrightarrow{25\%} 171$
	3	3.53	0.3984	2.4008	0.5972	1.20	$170 \xrightarrow{36\%} 172$
	4	3.66	0.3806	4.0709	0.0216	0.50	$169 \xrightarrow{23\%} 178$
	5	3.83	0.3534	1.9721	0.0526	1.43	$170 \xrightarrow{19\%} 176$
PPICN-Cz	1	0.55	0.47062	1.1576	0.0067	3.10	$172 \xrightarrow{88\%} 175$
	2	0.61	0.48113	1.0686	0.0008	1.66	$173 \xrightarrow{89\%} 178$
	3	0.84	0.45874	1.4100	0.0081	2.79	$174 \xrightarrow{92\%} 178$
	4	1.57	0.42863	1.2663	0.0603	1.87	$170 \xrightarrow{69\%} 175$
	5	1.59	0.39305	3.1415	0.0726	0.83	$174 \xrightarrow{32\%} 179$

Table S8: Computed excitation energy (eV), excitation coefficient, Δr (Å), oscillator strength (*f*) and dipolemoment (μ, D) for singlet states of PPI-An and PPICN-An.

Emitters	State	Excitation energy	Excitation coefficient	Δr	Oscillator strength	μ	NTO Transitions
PPI-An	1	2.64	0.4595	0.4388	0.2938	0.58	$146 \xrightarrow{73\%} 147$
	2	2.92	0.4491	3.1565	0.8180	0.92	$146 \xrightarrow{48\%} 148$
	3	3.02	0.4393	1.1199	0.0465	1.73	$143 \xrightarrow{43\%} 148$
	4	3.16	0.4005	2.4492	0.1084	1.41	$146 \xrightarrow{32\%} 149$
	5	3.32	0.4595	0.4388	0.0129	0.57	$146 \xrightarrow{32\%} 151$
PPICN-An	1	2.64	0.4591	0.4806	0.2933	0.61	$150 \xrightarrow{72\%} 151$
	2	2.92	0.4424	2.9787	0.8523	0.99	$150 \xrightarrow{35\%} 153$
	3	3.03	0.4386	1.3727	0.0387	1.84	$147 \xrightarrow{43\%} 153$
	4	3.17	0.4062	2.9545	0.1336	2.45	$150 \xrightarrow{29\%} 154$
	5	3.29	0.3679	2.5629	0.0910	0.64	$150 \xrightarrow{18\%} 152$

Table S9: Computed excitation energy (eV), excitation coefficient, Δr (Å), oscillator strength (*f*) and dipolemoment (μ, D) for singlet states of PPI-Py and PPICN-Py.

Emitters	State	Excitation energy	Excitation coefficient	Δr	Oscillator strength	μ	NTO Transitions
PPI-Py	1	2.89	0.4402	3.6710	1.7990	0.36	$154 \xrightarrow{50\%} 155$
	2	3.01	0.4152	2.6923	0.5615	0.44	$154 \xrightarrow{49\%} 156$
	3	3.24	0.3349	2.9493	0.1284	1.28	$153 \xrightarrow{18\%} 156$
	4	3.25	0.4160	2.6497	0.0221	0.53	$153 \xrightarrow{22\%} 155$
	5	3.26	0.3207	3.0665	0.0327	0.47	$151 \xrightarrow{29\%} 158$
PPICN-Py	1	2.89	0.4394	4.7259	1.7642	6.17	$158 \xrightarrow{35\%} 160$
	2	3.01	0.4259	3.6489	0.6147	5.64	$158 \xrightarrow{48\%} 161$
	3	3.23	0.3737	4.5599	0.2428	0.99	$158 \xrightarrow{19\%} 162$
	4	3.25	0.4001	2.6567	0.0232	0.79	$158 \xrightarrow{19\%} 162$
	5	3.25	0.3862	2.5888	0.0166	2.25	$158 \xrightarrow{19\%} 162$

Table S10: Computed RMSD of electron and hole, H index and t index for singlet states of PPI-Cz and PPICN-Cz.

Emitters	State	RMSD (Electron)				RMSD (Hole)				H index				t index			
		x	y	z	total	x	y	z	total	x	y	z	Total	x	y	z	Total
PPI-Cz	S1	2.634	2.622	0.779	3.797	2.995	2.964	0.792	4.287	2.814	2.793	0.786	4.042	-2.281	-2.445	-0.733	3.423
	S2	2.562	2.555	0.784	3.702	2.908	2.950	0.786	4.217	2.735	2.753	0.785	3.959	-2.442	-2.430	-0.770	3.530
	S3	1.939	1.440	1.410	2.796	2.549	1.475	1.267	3.206	2.244	1.458	1.338	2.992	-1.400	-1.413	-1.144	2.294
	S4	2.500	1.477	1.390	3.219	2.904	1.719	1.387	3.649	2.702	1.598	1.389	3.433	-2.339	-1.506	-1.306	3.073
	S5	4.001	3.123	0.871	5.150	3.655	2.720	0.822	4.630	3.828	2.921	0.847	4.889	-2.661	-2.851	-0.674	3.957
PPICN-Cz	S1	0.944	0.955	0.769	1.548	2.072	1.277	0.753	2.547	1.508	1.116	0.761	2.025	0.114	-0.331	-0.270	0.442
	S2	1.226	1.021	0.776	1.774	1.102	1.255	0.990	1.941	1.164	1.138	0.883	1.852	-0.441	-0.424	-0.674	0.910
	S3	0.898	0.947	0.748	1.505	1.800	1.378	0.720	2.378	1.349	1.162	0.734	1.926	0.097	-0.119	-0.334	0.368
	S4	1.387	2.578	0.807	3.036	1.866	2.539	0.779	3.246	1.626	2.558	0.793	3.134	-0.879	-1.633	-0.455	1.910
	S5	2.448	2.959	0.933	3.952	1.781	2.822	0.784	3.428	2.114	2.891	0.859	3.683	-1.985	-2.277	-0.775	3.118

Table S11: Computed RMSD of electron and hole, H index and t index for singlet states of PPI-An and PPICN-An

Emitters	State	RMSD (Electron)				RMSD (Hole)				H index				t index			
		x	y	z	total	x	y	z	total	x	y	z	Total	x	y	z	Total
PPI-An	S1	2.032	3.997	0.875	4.569	1.530	3.210	0.843	3.655	1.781	3.604	0.859	4.111	-1.640	-3.248	-0.776	3.720
	S2	2.165	4.244	0.924	4.853	1.556	3.256	3.256	3.707	1.861	3.750	0.884	4.279	-1.234	-3.603	-0.857	3.903
	S3	1.727	3.758	0.901	4.233	1.530	3.210	0.843	3.655	1.629	3.484	0.872	3.944	-0.685	-2.595	-0.733	2.782
	S4	2.969	2.952	0.834	4.269	1.729	3.388	0.846	3.897	2.349	3.170	0.840	4.034	-1.341	-2.503	-0.706	2.926
	S5	3.142	3.934	0.875	5.111	2.321	4.155	0.843	4.834	2.732	4.045	0.859	4.956	-2.581	-3.612	-0.797	4.510
PPICN-An	S1	2.127	3.954	0.990	4.597	1.515	3.193	0.923	3.653	1.821	3.574	0.957	4.123	-1.593	-3.243	-0.859	3.714
	S2	2.054	4.233	1.039	4.819	1.515	3.193	0.923	3.653	1.785	3.713	0.981	4.235	-1.100	-3.555	-0.920	3.833
	S3	1.915	3.700	1.020	4.289	1.515	3.193	0.923	3.653	1.715	3.446	0.972	3.970	-0.912	-2.326	-0.809	2.626
	S4	3.500	2.669	1.017	4.518	1.795	3.227	0.934	3.809	2.647	2.948	0.976	4.081	-0.618	-2.760	-0.880	2.962
	S5	3.313	3.865	0.968	5.182	2.248	3.920	0.906	4.609	2.781	3.893	0.937	4.875	-2.424	-3.510	-0.836	4.347

Table S12: Computed RMSD of electron and hole, H index and t index for singlet states of PPI-Py and PPICN-Py.

Emitters	State	RMSD (Electron)				RMSD (Hole)				H index				t index			
		x	y	z	total	x	y	z	total	x	y	z	Total	x	y	z	Total
PPI-Py	S1	4.775	4.520	0.705	6.613	4.518	4.231	0.713	6.231	4.647	4.376	0.709	6.422	-4.437	-4.274	-0.686	6.199
	S2	4.903	3.472	0.699	6.049	4.734	3.366	0.713	5.852	4.819	3.419	0.706	5.950	-4.534	-3.319	-0.678	5.659
	S3	4.324	4.778	0.783	6.491	4.290	4.347	0.709	6.148	4.307	4.562	0.746	6.318	-3.206	-4.558	-0.710	5.618
	S4	3.540	2.414	0.678	4.338	3.858	2.518	0.706	4.661	3.699	2.466	0.692	4.499	-3.339	-2.406	-0.677	4.171
	S5	3.733	4.330	0.730	5.763	3.435	3.446	0.594	4.902	3.584	3.888	0.662	5.329	-3.384	-3.505	-0.598	4.908
PPICN-Py	S1	4.749	4.504	0.723	6.585	4.638	4.267	0.725	6.344	4.694	4.386	0.724	6.465	-4.303	-4.275	-0.718	6.108
	S2	4.872	3.340	0.714	5.950	4.608	3.297	0.732	5.713	4.740	3.318	0.723	5.831	-4.693	-2.832	-0.704	5.526
	S3	2.905	4.882	0.797	5.737	3.284	4.080	0.732	5.288	3.095	4.481	0.765	5.499	-0.766	-2.452	-0.764	2.680
	S4	3.904	2.503	0.703	4.691	3.941	2.484	0.735	4.716	3.923	2.493	0.719	4.703	-3.808	-2.432	-0.703	4.572
	S5	3.349	3.982	0.730	5.254	3.534	3.867	0.722	5.288	3.441	3.924	0.726	5.270	-2.878	-3.741	-0.705	4.772

Table S13. Computed hole and electron overlap (S), distance between centroids of hole and electron (D, Å) and dipolemoment (μ) for singlet states of PPI-Cz and PPICN-Cz.

Emitters	State	Hole integral	Electron integral	Integral of transition density	Integral overlap of h^+- e^- (S)	Centroid of hole (Å)			Centroid of electron (Å)			D (Å)	μ (a.u)
						x	y	z	x	y	z		
PPI-Cz	S1	0.7525	0.5694	-0.0008	0.4105	-0.8571	-0.2758	0.0775	-1.3902	-0.6238	0.0244	0.6388	0.7980
	S2	0.7113	0.5452	-0.0023	0.2521	-1.1280	-0.5652	0.2499	-1.4207	-0.2422	0.2651	0.4361	0.5178
	S3	0.8311	0.6360	-0.0148	0.5008	-5.7770	1.1974	0.1429	-6.6209	1.1526	0.3377	0.8672	1.2022
	S4	0.8091	0.5734	-0.0005	0.3910	-5.8132	1.1163	0.1957	-6.1761	1.2081	0.2783	0.3833	0.5008
	S5	0.7259	0.5570	-0.0081	0.3385	-1.2190	-1.1530	0.2952	-2.3864	-1.0827	0.1224	1.1822	1.4332
PPICN-Cz	S1	0.9260	0.8306	0.0295	0.1563	5.0523	3.5413	0.4267	6.6742	4.3260	-0.0643	1.8674	3.0997
	S2	0.8783	0.8198	0.0064	0.2677	7.1784	-2.3760	0.0266	7.9012	-1.6621	0.2359	1.0371	1.6642
	S3	0.8306	0.7831	-0.0016	0.3083	6.5779	-2.6614	-0.1321	8.0242	-1.6179	0.2682	1.8278	2.7870
	S4	0.8518	0.7497	-0.0084	0.3522	5.8628	2.4269	0.2531	6.6102	3.3523	-0.0852	1.2367	1.8715
	S5	0.7294	0.6647	0.0060	0.3281	6.4611	-1.3069	-0.0131	6.5907	-0.6933	-0.0965	0.6327	0.8335

Table S14. Computed hole and electron overlap (S), distance between centroids of hole and electron (D, Å) and dipolemoment (μ) for singlet states of PPI-An and PPICN-An.

Emitters	State	Hole integral	Electron integral	Integral of transition density	Integral overlap of h^+- e^- (S)	Centroid of hole (Å)			Centroid of electron (Å)			D (Å)	μ (a.u)
						x	y	z	x	y	z		
PPI-An	S1	0.8031	0.7620	0.0024	0.39176	3.9365	0.6275	-0.0714	3.7956	0.2712	-0.1546	0.3920	0.5798
	S2	0.7873	0.7222	-0.0241	0.25060	3.9160	0.6450	-0.0714	4.5431	0.7926	-0.0440	0.6447	0.9197
	S3	0.7678	0.6368	0.0076	0.21810	3.9365	0.6275	-0.0714	4.8798	-0.2616	-0.2102	1.3037	1.7303
	S4	0.7089	0.5185	0.0396	0.25036	3.8037	0.4502	-0.1070	2.7958	1.1166	0.0276	1.2157	1.4101
	S5	0.7014	0.6155	-0.0102	0.39870	2.6678	1.4608	-0.0479	2.8185	1.0277	-0.1095	0.4626	0.5757
PPICN- An	S1	0.8014	0.7611	-0.0026	0.3868	4.1224	0.4474	-0.0514	3.8940	0.1167	-0.1492	0.4135	0.6105
	S2	0.7723	0.7133	-0.0279	0.2350	4.1224	0.4474	-0.0514	4.8067	0.6056	0.0094	0.7050	0.9897
	S3	0.7656	0.6354	0.0064	0.2144	4.1224	0.4474	-0.0514	4.9256	0.6732	-0.2145	1.3883	1.8379
	S4	0.7149	0.5553	-0.0300	0.2217	4.1224	0.3206	-0.0781	1.9269	0.5084	0.0181	2.0400	2.4485
	S5	0.6781	0.5887	0.0200	0.3909	3.2074	1.7136	0.0217	2.8512	1.3312	-0.0793	0.5323	0.6372

Table S15. Computed hole and electron overlap (S), distance between centroids of hole and electron (D, Å) and dipolemoment (μ) for singlet states of PPI-Py and PPICN-Py.

Emitters	State	Hole integral	Electron integral	Integral of transition density	Integral overlap of h^+- e^- (S)	Centroid of hole (Å)			Centroid of electron (Å)			D (Å)	μ (a.u)
						x	y	z	x	y	z		
PPI-Py	S1	0.8935	0.7392	0.0039	0.5904	0.7264	2.8450	-0.0421	0.5171	2.7430	-0.0190	0.2340	0.3610
	S2	0.8445	0.6970	-0.0017	0.5686	4.7985	0.2374	-0.0226	5.0830	0.1371	0.0054	0.3030	0.4413
	S3	0.6914	0.5349	-0.0068	0.3873	0.3021	2.6139	-0.0537	-0.7986	2.6096	-0.0179	1.1013	1.2761
	S4	0.8776	0.6515	-0.0010	0.5468	6.6156	-0.6428	0.0163	6.9755	-0.5826	0.0310	0.3651	0.5276
	S5	0.6109	0.5235	-0.0042	0.3025	-1.0973	3.3245	-0.0909	-1.2974	3.7081	-0.0267	0.4373	0.4688
PPICN-Py	S1	0.8938	0.7370	0.0046	0.59417	1.2128	2.8846	-0.0826	0.8223	2.7733	-0.0762	0.4060	0.6257
	S2	0.8682	0.7152	0.0008	0.57016	5.2887	0.0342	0.0113	5.3361	-0.4518	0.0300	0.4888	0.7313
	S3	0.7632	0.6168	-0.0131	0.30408	0.1630	0.8140	-0.2433	-2.1654	-1.2152	-0.2444	3.0886	4.0279
	S4	0.8454	0.6277	0.0001	0.54633	6.6886	-0.7453	0.0730	6.8036	-0.6840	0.0887	0.1313	0.1827
	S5	0.8166	0.6084	0.0023	0.5132	-0.6419	4.6308	-0.0900	-1.20586	4.8139	-0.0693	0.5932	0.7988